

Effects of mouse ovarian tissue cryopreservation on granulosa cell–oocyte interaction

P.Navarro-Costa¹, S.C.Correia², A.Gouveia-Oliveira³, F.Negreiro³, S.Jorge², A.J.Cidadão¹, M.J.Carvalho² and C.E.Plancha^{1,4}

¹Biology of Reproduction Unit, Institute of Molecular Medicine, Lisbon Medical School, 1649-028 Lisboa, ²Medicine of Reproduction Unit, Gynaecology Service, Maternidade Dr. Alfredo da Costa, 1069–089 Lisboa and ³Datamedica Lda., Rua Rosa Araújo, 34, 5º, 1250–195 Lisboa, Portugal

⁴To whom correspondence should be addressed. E-mail: carlos.plancha@mail.telepac.pt

BACKGROUND: Current ovarian tissue cryopreservation protocols have yet to be assessed in terms of somatic–germ cell interaction. Accordingly, post-thaw analysis of antral follicles can yield relevant data on the disruption of the granulosa–oocyte interface. **METHODS:** We compared fresh mouse ovarian tissue with tissues that had been either cryopreserved using dimethylsulphoxide (DMSO) or glycerol as cryoprotectants, or exposed to such cryoprotectants without freezing. The assessed parameters were: number of immature oocytes retrieved per ovary, allocation of the oocytes to different classes regarding antral follicle size and oocyte–granulosa cell adhesion, and the relative density of transzonal processes containing filamentous actin (TZPs-Act). **RESULTS:** Although cryopreservation reduces the average number of oocytes retrieved per ovary, it increases the relative distribution of granulosa-free oocytes while decreasing that of granulosa-enclosed ones. Additionally, a post-thaw decrease in TZPs-Act density was recorded. This decrease was also observed after cryoprotectant exposure without freezing, although at a lower level. For the assessed parameters, DMSO was more effective than glycerol as a cryoprotectant. **CONCLUSIONS:** *In situ* cryopreservation of granulosa–oocyte complexes with current protocols disrupts the granulosa–oocyte interface. The different patterns of granulosa cell adhesion and interaction in oocytes derived from different-sized antral follicles further suggests that the granulosa–oocyte interface may be developmentally regulated.

Key words: actin/granulosa–oocyte communication/ovarian tissue cryopreservation/transzonal processes

Introduction

Bi-directional interactions between developing germ cells and their somatic neighbours are crucial for the fertility of a wide range of species (Albertini and Rider, 1994; Deng and Lin, 2001; Eppig *et al.*, 2002; Matzuk *et al.*, 2002). The mammalian oocyte maintains a close structural relationship with granulosa cells spanning from follicle formation to ovulation (Albertini and Rider, 1994; Hertig and Adams, 1967). Accordingly, the regulation of follicular development is dependent on the granulosa–oocyte interface (Buccione *et al.*, 1990; Albertini *et al.*, 2001; for a review see also Gilchrist *et al.*, 2004). In the ovarian follicle, somatic cell proliferation and differentiation are oocyte-controlled, while germ cell development, meiotic progression and global transcriptional pattern are regulated by granulosa cells (Matzuk *et al.*, 2002). Furthermore, antral stages of follicular development and oocyte maturation were shown to be dependent on somatic–germ cell communication via gap junctions (Simon *et al.*, 1997; Carabatsos *et al.*, 2000), which supports the view that during follicular development considerable

amounts of metabolites are exchanged in the granulosa–oocyte interface (Pellicer *et al.*, 1988). Part of the granulosa–oocyte communication is mediated by transzonal projections (TZPs) emanating from neighbouring granulosa cells (Anderson and Albertini, 1976). These TZPs have to navigate the zona pellucida mesh, taking irregular, sometimes even bifurcated routes, before establishing contact with the oocyte's surface (Anderson and Albertini, 1976). In this regard, TZPs are finely regulated dynamic structures that respond either to developmental (Motta *et al.*, 1994) or hormonal (Combelles *et al.*, 2004) stimuli. It is assumed that bi-directional information exchange between the oocyte and granulosa cells implies dynamic alterations in the number and form of TZPs in a developmental stage-dependent manner (Motta *et al.*, 1994; Albertini and Barrett, 2003). Additionally, TZPs are thought to be heterogeneous with respect to cytoskeletal content (Albertini and Rider, 1994): they can be sustained by filamentous actin (TZPs-Act), microtubules (TZPs-MT) or both. Whereas TZPs-MT are characterized by a helical conformation, TZPs-Act take

a more perpendicular course through the zona pellucida (Albertini and Rider, 1994). Nevertheless, both types of organization ensure the shape and motility of the TZP, serving as a dynamic scaffold for the structure. Although there are few studies characterizing TZPs-Act, it was shown that they could vary significantly between different species and in the degree of penetration in the zona pellucida (Albertini and Rider, 1994; Albertini and Barrett, 2003). The type of contact established between the TZP and the oocyte's membrane can take one of two forms. Accordingly, different types of adherens (Zamboni, 1974; Motta *et al.*, 1994) as well as gap junctions (Anderson and Albertini, 1976) have already been characterized, further illustrating the importance of cell adhesion and communication in the granulosa–oocyte interface.

Ovarian tissue cryopreservation is more effective in terms of follicle survival and blastocyst formation from recovered oocytes than cryopreserving isolated follicles (Correia *et al.*, 1999). Therefore, it seems that the follicular structure is more resilient to cryo-induced damage when integrated in the ovarian tissue. Recent advances in whole ovary cryopreservation and transplantation seem to support this view (Wang *et al.*, 2002). Nevertheless, the low success of tissue cryopreservation when compared to that of single cells is thought to be due partially to the detrimental effect exerted by low temperatures upon cellular interactions. Ovarian tissue cryopreservation has been mostly analysed in terms of follicle survival after thawing. It is documented that only primordial or small preantral follicles survive cryo-induced damage (Hovatta *et al.*, 1996; Oktay *et al.*, 1997; Gook *et al.*, 1999, 2001). However, this is probably not a direct consequence of cryo-induced damage, but the result of the lack of post-graft vascularization of antral and large preantral follicles. In accordance, oocytes recovered from antral follicles of cryopreserved murine ovaries have been shown to survive the cryopreservation protocol and sustain full developmental competence after *in vitro* maturation and fertilization (Sztejn *et al.*, 2000). This suggests that post-thaw antral follicles can yield relevant data on the possible disruption of cellular communication routes in the follicle as a consequence of cryo-induced damage.

Taking into account the importance of granulosa–oocyte communication in the follicle, this study aimed to investigate for the first time the possible deleterious effects resulting from cryo-injury and cryoprotectant exposure without freezing on TZPs-Act. The correlation between antral follicle size and the status of the oocyte–granulosa cell interface was also characterized. Specifically, the assessed parameters on fresh, cryoprotectant-exposed and cryopreserved ovarian tissue were: average number of oocytes collected per ovary, allocation of oocytes to different classes regarding antral follicle size and granulosa–oocyte cell adhesion, and relative density of TZPs-Act.

Materials and methods

Oocyte retrieval, scoring and fixation

Eight to ten-week old F1 (CBA × C57BL/6) female mice were bred from stock (Harlan, Spain) and kept under controlled light

(14h light, 10h dark) and temperature (25°C) conditions. They were fed pellets (Panlab, Spain) and acidified water, *ad libitum*. Superovulation was induced by interperitoneal injection of 0.1 ml pregnant mare serum gonadotrophin (PMSG), 50 IU/ml (Intervet, Portugal), and 44–48 h later the animals were euthanized by cervical dislocation. The ovaries were immediately removed and placed in minimum essential medium (MEM) with Earle's salts, 25 mmol/l HEPES, without L-Glu (Gibco, UK) supplemented with 50 IU/ml penicillin and 50 mg/ml streptomycin (Gibco, UK), at 37°C. Adipose tissue was thoroughly removed from the ovaries (average size: 2.4 × 3.4 × 1.7 mm). The contents of large antral follicles were released in a new Petri dish containing fresh MEM at 37°C by selective puncture of antral follicles with a hypodermic needle (0.50 × 16 mm) (Braun, Germany). In a preliminary assay, we established that only follicles with a diameter >300 µm were large enough to be individually identified and punctured. The released germinal vesicle (GV) stage oocytes were scored for granulosa–oocyte cell adhesion as previously described (Combelles and Albertini, 2003): C^{A+} for granulosa-enclosed oocytes, C^{A+/-} for partially granulosa-enclosed oocytes (whenever there were granulosa cell-free regions on the oocyte surface) and C^{A-} for granulosa-free oocytes. The suffix 'A' indicates that the oocytes were retrieved from large antral follicles. The total number of oocytes retrieved and the number of oocytes for each experimental class was recorded. After separating the oocytes, all granulosa cells were removed by gentle pipetting with a pulled Pasteur pipette, and the oocytes were fixed overnight as previously described (Plancha, 1996) at 4°C in 3.7% paraformaldehyde (PFA).

This procedure was repeated in a new Petri dish containing fresh MEM at 37°C for the retrieval of oocytes enclosed in small antral follicles. In this case, ovaries were randomly punctured. C^{a+}, C^{a+/-} and C^{a-} classes were established, as above, with the suffix 'a' indicating that the oocytes were retrieved from small antral follicles.

Oocytes derived both from large and small antral follicles had an identical average diameter of 75 µm (excluding zona pellucida), further confirming that they were fully grown.

Exposure of ovarian tissue to cryoprotectant solutions without freezing

Freshly collected ovaries were dissociated from adipose tissue in MEM and transferred to a Petri dish containing cryoprotectant solution at 4°C consisting of either 1.5 mol/l dimethylsulphoxide (DMSO; Merck, Germany) or 1.5 mol/l glycerol (Sigma–Aldrich, Germany), diluted in Leibovitz medium (Gibco, UK) supplemented with 10% fetal bovine serum (FBS) heat-inactivated and 0.1 mol/l sucrose (Sigma–Aldrich, Germany). After a 30 min exposure to the cryoprotectant solution, the ovaries were transferred to an initial cryoprotectant-dilution solution for 5 min at 37°C, consisting of Leibovitz supplemented with 10% FBS heat-inactivated, 50 IU/ml penicillin, 50 mg/ml streptomycin, 0.1 mol/l sucrose, and 1 mol/l DMSO or glycerol, accordingly. This step was repeated twice with cryoprotectant-dilution solutions of decreasing molarity (DMSO or glycerol first at 0.5 mol/l and then at 0.1 mol/l, for 5 min each). The ovaries were then transferred for another 5 min to a Petri dish containing fresh medium at 37°C consisting of Leibovitz supplemented with 10% FBS heat-inactivated, 50 IU/ml penicillin and 50 mg/ml streptomycin. Following cryoprotectant dilution, the ovaries were processed according to the oocyte retrieval, scoring and fixation protocol. The total number of oocytes retrieved and the number of oocytes for each experimental class was recorded.

Cryopreservation of ovarian tissue

Slow freezing

Freshly collected ovaries were thoroughly dissociated from adipose tissue in MEM and transferred to a Petri dish containing cryoprotectant solution at 4°C consisting of 1.5 mol/l DMSO diluted in Leibovitz medium supplemented with 10% FBS heat-inactivated and 0.1 mol/l sucrose. An alternative cryoprotectant solution was also tested with 1.5 mol/l glycerol instead of DMSO. In both cryopreservation groups, a linear perforation on the ovary's main axis was performed with a hypodermic needle in order to ensure proper permeation of the cryoprotectant solution. After a 30 min exposure to the cryoprotectant solution, the ovaries were transferred to the cryotubes (Nunc 1.0 ml conical, Co. no. 366656, Denmark) containing the DMSO or glycerol cryoprotectant solution. A slow cooling protocol was performed in a controlled-rate freezer (Biomed Freezer Kryo10; Planer, UK). The cryotubes were placed in the controlled-rate freezer that had been precooled to 4°C, and cooling was performed at $-2^{\circ}\text{C}/\text{min}$ to -5°C . The samples were held at -5°C for 10 min to ensure temperature equilibration, and then were manually seeded. Cooling was then continued at the rate of $-0.3^{\circ}\text{C}/\text{min}$ to -40°C , and finally at $-10^{\circ}\text{C}/\text{min}$ to -100°C . When the samples reached the temperature of -100°C , the cryotubes were removed from the controlled-rate freezer and plunged in liquid nitrogen. The cryotubes were stored at -196°C for a minimum of a week.

Multi-step rapid thawing

The cryotubes were removed from liquid nitrogen storage and plunged in a 27°C water bath. When the contents of the cryotubes appeared unfrozen (after ~ 2 min at 27°C), the ovaries were transferred to a cryoprotectant-dilution solution at 37°C consisting of Leibovitz supplemented with 10% FBS heat-inactivated, 50 IU/ml penicillin, 50 mg/ml streptomycin, 0.1 mol/l sucrose and 1 mol/l DMSO or glycerol, accordingly. After 5 min, this step was repeated twice with cryoprotectant-dilution solutions of decreasing molarity (DMSO or glycerol first at 0.5 mol/l and then at 0.1 mol/l, for 5 min each). The ovaries were then transferred for another 5 min to a Petri dish containing fresh medium at 37°C consisting of Leibovitz supplemented with 10% FBS heat-inactivated, 50 IU/ml penicillin and 50 mg/ml streptomycin. The ovaries were finally processed according to the oocyte retrieval, scoring and fixation protocol. The total number of oocytes retrieved and the number of oocytes for each experimental class was recorded.

Oocyte assessment

Microfilaments staining

Both fresh and cryopreserved oocytes were stained for filamentous actin (f-actin). Oocytes were transferred from the fixative to 60-well plates (Nunc, Co. number 163118, Denmark) containing 10 μl of wash solution consisting of phosphate-buffered saline (PBS) supplemented with 0.05% (v/v) Tween 20 (Sigma–Aldrich, Germany). The 15 min wash was repeated twice. Oocytes were then incubated for 30 min at room temperature in phalloidin–tetramethylrhodamine B isothiocyanate (TRITC; Sigma, USA). Afterwards, the oocytes were washed thrice in the dark, 15 min each, in the appropriate solution. Oocytes were placed on a glass slide in a droplet of 1,4-diazobicyclo(2,2,2)-octane (DABCO) medium supplemented with sodium azide (Sigma–Aldrich, Germany). The droplet was delimited by a DAKO pen ring (Dakopatts, Denmark) and the cover slip was placed so as to be supported by four glass towers in order to preserve the oocyte's volume. The mounted oocytes were stored in the dark at 4°C until visualization by fluorescence microscopy.

Computerized analysis of the fluorescence signal

Since direct analysis of individual TZPs is only possible in electron or confocal microscopy, an indirect analysis was performed. Images of the equatorial planes of the oocytes were captured using an optical fluorescence microscope (Leica DMR, Germany) with a fitted camera (Leica DC350F, Germany). The software used was Leica DC Twain version 4.1 (Leica Microsystems, Germany) and Adobe Photoshop version 6.0 (Adobe Systems Inc., USA). The grayscale images were then analysed for the intensity of the fluorescence signal emanating from the zona pellucida, where the TZPs–Act are located. The software used was ImageTool version 3.0 (University of Texas Health Science Centre in San Antonio, USA) and the analysis was based on an algorithm that calculated the distribution of the grayscale values in the number of pixels of the selected region. The regions had $\sim 300\,000$ pixel², and four regions were selected in the zona pellucida of each oocyte so as to obtain a representative average of that oocyte. In order to calibrate this value, the average was further divided by cytoplasmic actin-f fluorescence intensity. Thus, the resulting image ratios correspond to relative intensities of the fluorescence signal.

Statistical analysis

For the fresh, cryopreservation in DMSO and cryopreservation in glycerol groups, a minimum of 31 ovaries per group was used. For the two cryoprotectant exposure groups, a minimum of 16 ovaries per group was used. The effects of cryopreservation protocols, freezing, and their interaction on the number of retrieved oocytes were estimated by a linear regression model. To test for shifts between the experimental groups in the number of oocytes allocated to different classes of granulosa cell adhesion, a multinomial logistic regression model of oocyte class on cryopreservation protocol and freezing, adjusted for follicle size, was used.

The differences between experimental groups in the average number of retrieved oocytes and in the relative intensity of the phalloidin–TRITC signal were tested with fixed-effects ANOVA models with Bonferroni correction for multiple comparisons. The effects of follicle size, cryopreservation protocol, and freezing on the relative intensity of the phalloidin–TRITC signal were estimated with a multiple linear regression model. A subsequent model tested the interaction between the cryopreservation protocol and freezing on the signal intensity, adjusting for follicle size. All statistical analyses were performed with Stata release 7.0 (Stata Corporation, USA).

Results

Cryopreservation reduces the average number of oocytes retrieved per ovary

The average number of GV stage oocytes retrieved per ovary was assessed in fresh tissue, after cryopreservation of whole ovaries, and after exposing whole ovaries to the cryoprotectant solutions without freezing. In fresh tissue, an average of 16.43 oocytes was retrieved per ovary. This average significantly decreased after cryopreservation to 10.68 and 9.19 oocytes in DMSO and glycerol protocols respectively ($P = 0.008$ and $P < 0.001$; Figure 1)

Exposing whole ovaries to the cryoprotectant solutions without freezing had a different effect depending on whether DMSO or glycerol was used. Specifically, exposure to DMSO did not alter the average number of oocytes retrieved per ovary (15.38) when compared to fresh tissue, while

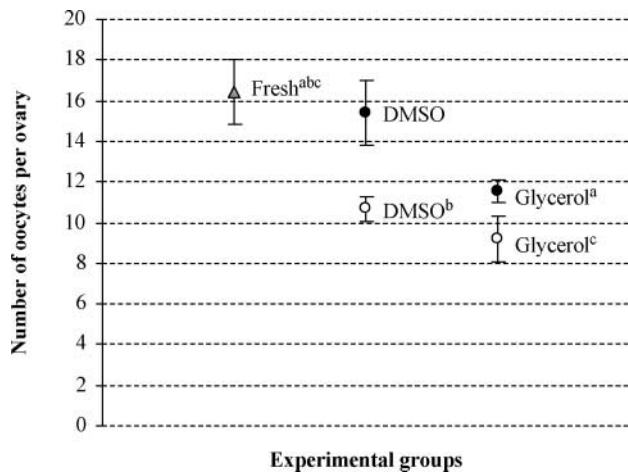


Figure 1. Average number of oocytes retrieved per murine ovary between the different experimental groups. Whole ovaries were exposed to the cryoprotectant solutions without freezing (●) or cryopreserved in the corresponding solutions (○). Fresh tissue is also represented (▲). Results are expressed as mean ± SEM. Same superscript indicates statistically significant difference (one-way ANOVA with multiple comparison tests, $P < 0.05$). Sample size: 126 ovaries.

exposure to glycerol led to a significant reduction to 11.56 oocytes ($P = 0.031$; Figure 1).

Cryopreservation of whole ovaries markedly decreases the recovery of granulosa-enclosed oocytes

Oocytes retrieved from fresh ovaries show different patterns of association with granulosa cells whether they were derived from large or small antral follicles. Specifically, in oocytes derived from large antral follicles, there is a clear predominance of granulosa-enclosed oocytes (C^{A+}) against granulosa-free oocytes (C^{A-} ; $P < 0.001$). Yet, in oocytes derived from small antral follicles, the three granulosa cell classes show a similar percentage of oocytes (Figure 2).

In contrast, oocytes recovered from cryopreserved ovaries exhibited a significantly higher percentage of granulosa-free classes when compared to those recovered from the fresh tissue ($P < 0.001$). This effect was detected in oocytes derived both from large and small antral follicles. Accordingly, C^{A-} oocytes increase sharply from 20% in the fresh tissue to 63 and 58% after cryopreservation in DMSO and glycerol respectively. Likewise, C^{a-} oocytes increase from 36% in the fresh tissue to 67 and 78% after cryopreservation in DMSO and glycerol respectively (Figure 2). On the other hand, post-thaw ovaries exhibit a marked decrease in the percentage of the granulosa-enclosed classes (C^{A+} and C^{a+}) when compared to those recovered from the fresh tissue ($P = 0.011$). Again, this effect was detected in oocytes derived both from large and small antral follicles. No significant differences between cryopreservation in DMSO and glycerol were detected in the allocation of oocytes to the different classes.

Exposing whole ovaries to the cryoprotectant solutions without freezing had a different effect depending on whether DMSO or glycerol was used. Specifically, DMSO did not

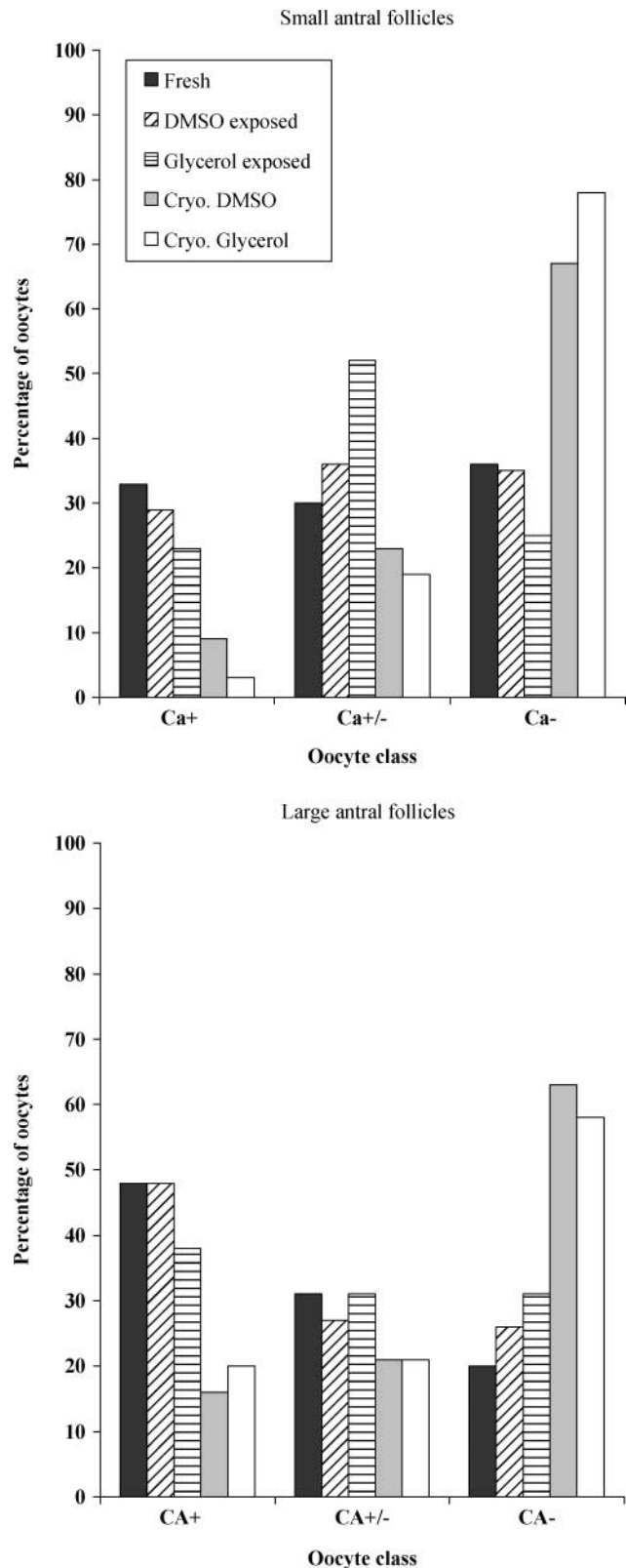


Figure 2. Percentage of murine germinal vesicle stage oocytes, scored for granulosa–oocyte adhesion, derived from small or large antral follicles. Statistically significant difference is indicated in the text, as statistical analysis was performed using a multinomial regression model with pooled data. Sample size: 1564 oocytes.

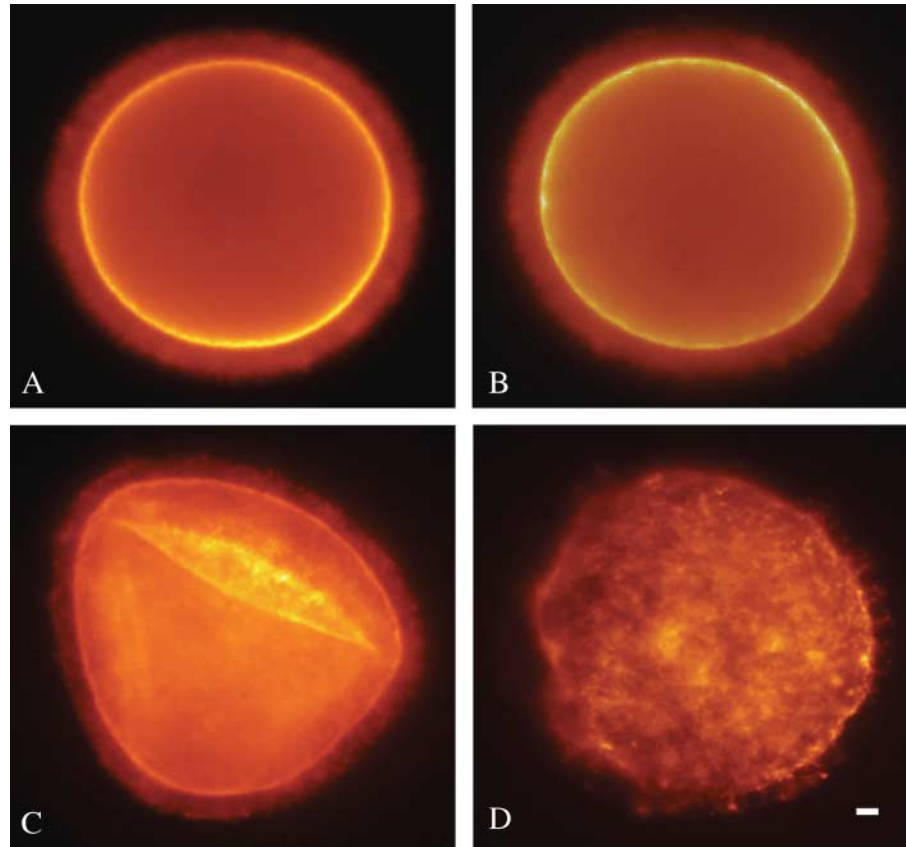


Figure 3. Fluorescence micrographs of murine germinal vesicle stage oocytes stained with phalloidin–tetramethylrhodamine B isothiocyanate (bar = 10 μm). (A) Oocyte retrieved from fresh tissue, with the cortical f-actin network clearly visible. Zona pellucida staining reflects transzonal processes containing filamentous actin density. (B) Oocyte retrieved from ovarian tissue exposed to dimethylsulphoxide (DMSO) without freezing. A pattern similar to that of fresh control can be observed. (C) Oocyte retrieved from ovarian tissue cryopreserved in glycerol showing changes in oocyte volume and shape. (D) Oocyte retrieved from ovarian tissue cryopreserved in DMSO showing a partial collapse of the f-actin component.

alter the granulosa–oocyte cell adhesion pattern observed in the fresh tissue. In contrast, the glycerol solutions led to significant pattern modifications ($P < 0.05$). In particular, $C^{a+/-}$ oocytes increased from 30% in the fresh tissue to 52% after exposure to the glycerol solutions (Figure 2).

Cryopreservation of whole ovaries leads to TZPs-Act relative signal reduction

The filamentous actin staining in oocytes retrieved from fresh ovarian tissue revealed the expected pattern (Figure 3A) of ooplasm staining, prominent staining of the cortical f-actin network and radial staining in the zona pellucida, corresponding to the intricate mesh of TZPs-Act. The relative intensity of the microfilament signal is a positively correlated estimator of TZPs-Act density. Oocytes derived from large antral follicles showed a significant increase in the relative intensity of the microfilaments signal as they became more associated with granulosa cells from C^{A-} to C^{A+} ($P < 0.001$; Figure 4). The relative intensity was thus minimal for the C^{A-} class. Interestingly, no statistically significant difference was observed in oocytes retrieved from small antral follicles.

The filamentous actin staining pattern observed in fresh tissue was largely maintained after exposure to the cryoprotectant solutions without freezing (Figure 3B). In contrast,

cryopreservation clearly altered the staining pattern observed in fresh oocytes by introducing changes in cell volume and shape and deformations at the cortical f-actin network (Figure 3C and 3D). The extent of these post-thaw alterations

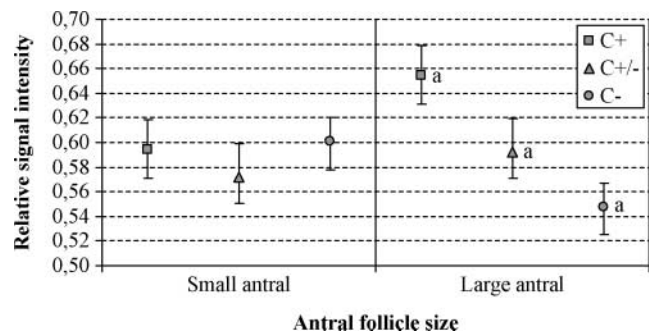


Figure 4. Relative intensity of the transzonal processes containing filamentous actin (TZPs-Act) fluorescence signal in murine oocytes with different types of granulosa–oocyte cell adhesion, scored for antral follicle size. C^+ stands for granulosa–oocyte cell adhesion, $C^{+/-}$ for partially granulosa–oocyte cell adhesion, and C^- for granulosa-free oocytes. Results are expressed as mean \pm SEM. Same superscript indicates statistically significant difference (multinomial regression model, $P < 0.05$). Sample size: 1220 oocytes.

Table I. Relative intensity of the fluorescence signal for murine oocytes derived from small and large antral follicles, scored for granulosa–oocyte adhesion

Follicle size	Oocyte class	Relative signal intensity per experimental group				
		Fresh	DMSO-exposed	Glycerol-exposed	Cryo DMSO	Cryo glycerol
Small antral	C ^{a+}	0.62	0.56	0.63	0.53	0.57
	C ^{a+/-}	0.61	0.55	0.56	0.55	0.55
	C ^{a-}	0.68	0.64	0.59	0.61	0.54
Large antral	C ^{A+}	0.69	0.65	0.65	0.62	0.58
	C ^{A+/-}	0.63	0.58	0.59	0.60	0.52
	C ^{A-}	0.53	0.56	0.53	0.56	0.54

Sample size: 1220 oocytes; statistical difference is indicated in Figures 4 and 5.

varied among the different cells analysed, as there were cryopreserved cells that retained the fresh pattern.

Cryopreservation significantly reduced relative signal intensity compared to fresh tissue, indicating partial disruption of TZPs-Act irrespective of antral follicle size ($P = 0.001$). Interestingly, this post-thaw reduction was not observed in the C^{A-} class, as it exhibited a relative signal intensity close to that of fresh tissue (Table I). Overall, the relative signal intensity was significantly lower in oocytes recovered from ovaries frozen in glycerol compared to those frozen in DMSO ($P < 0.005$), indicating that DMSO preserved TZPs-Act more efficiently than glycerol (Figure 5). A positive interaction between cryopreservation and both cryoprotectants was detected ($P = 0.048$).

Exposure of whole ovaries to the cryoprotectant solutions without freezing resulted in a significant reduction of the relative signal intensity when compared to fresh tissue ($P < 0.001$ for both the DMSO and glycerol solutions) (Figure 5). Although no significant differences in terms of

relative signal intensity were detected between exposures to DMSO and glycerol solutions, the same did not apply when exposure to cryoprotectant solutions was compared to the respective cryopreservation protocol. Specifically, cryopreservation in glycerol significantly reduced relative signal intensity when compared to exposure to glycerol without freezing ($P < 0.001$). In contrast, cryopreservation in DMSO maintained the relative signal intensity obtained with DMSO exposure without freezing.

Discussion

The results of this study indicate that cryopreserving ovarian tissue either in DMSO or in glycerol interferes with the granulosa–oocyte interface. Not only was there a post-thaw reduction of granulosa cell adhesion to the oocyte, as recently suggested in the cryopreservation of halved ovaries (Sztejn *et al.*, 2000) and isolated cumulus–oocyte complexes (COCS; Ruppert-Lingham *et al.*, 2003), but also a clear decrease in cell interaction via TZPs-Act is documented for the first time. Current cryopreservation protocols appear thus to affect crucial interactions between the oocyte and granulosa cells. Although DMSO seems to more effectively maintain the granulosa–oocyte interface than glycerol, further improvement of cryopreservation protocols, both at the freezing and cryoprotectant exposure stages, is still necessary to minimize the disruption of cellular communication routes in immature COCS. Given that oocyte maturation depends on the integrity of oocyte–granulosa interactions (Plancha and Albertini, 1994; Simon *et al.*, 1997; Carabatsos *et al.*, 2000; Matzuk *et al.*, 2002), this work may thus be of significance for future studies on cryopreservation of immature oocytes and oocyte maturation.

It is known that fresh tissue oocytes derived from follicles at different developmental stages show physiological differences regarding meiotic and somatic cell adhesion status (Gilchrist *et al.*, 1995). In the present study, fresh tissue oocytes exhibited different patterns of granulosa cell adhesion and interaction as they derived from large or small antral follicles. One might speculate that these patterns exhibited by the fresh tissue oocytes may reflect their developmental stage. In small antral follicles, the even distribution of oocytes between the classes may indicate that granulosa cell adhesion might become more pronounced only at later

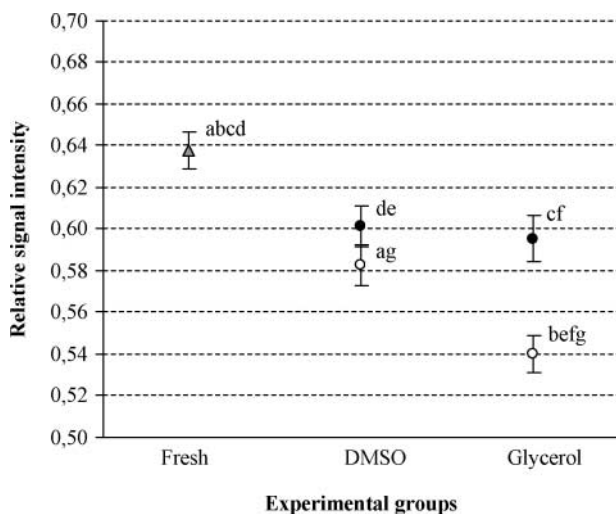


Figure 5. Relative intensity of the transzonal processes containing filamentous actin fluorescence signal of murine oocytes between the different experimental groups. Whole ovaries were exposed to the cryoprotectant solutions without freezing (●) or cryopreserved in the corresponding solutions (○). Fresh tissue is also represented (▲). Results are expressed as mean ± SEM. Same superscript indicates statistically significant difference (one-way ANOVA with multiple comparison tests, $P < 0.05$). Sample size: 1220 oocytes.

stages of follicular development. This way, the documented favouring of the granulosa-enclosed class in large antral follicles may be developmentally relevant, since the oocyte is ovulated as a COC. In fact, the retrieval of granulosa-free oocytes from antral follicles indicates that the progressive granulosa cell adhesion models for oocyte growth (Combelles and Albertini, 2003; Combelles *et al.*, 2004) may be more complex than previously thought. Accordingly, it is known that in human follicles larger than 1 mm, atresia is characterized by the oocyte persisting long after granulosa cells have disappeared (Gougeon, 1996). Thus, we hypothesize that the C^- class may contain oocytes that are entering the apoptotic pathway, and the $C^{+/-}$ class could represent initial stages of the same pathway.

In the present study, cryopreservation decreased the average number of oocytes retrieved per ovary. This result was to be expected probably due to inadequate cryoprotectant permeation in the antral follicle which may have compromised the oocyte's integrity during the cryopreservation protocol. Furthermore, possible intrafollicular ice formation at the antral cavity could have increased the oocyte lysis rate. Although the average number of oocytes retrieved per ovary decreased after cryopreservation, the percentage of granulosa-free oocytes derived either from large or small antral follicles significantly increased. This increase could have resulted from a shift of oocytes from the granulosa-enclosed classes to the granulosa-free ones. Two different mechanisms can be hypothesized to account for this cryo-induced damage: the increase in granulosa-free oocytes could result from the massive disruption of granulosa cell adhesion to the oocyte, denuding it directly to C^- . Alternatively, a more gradual denuding mechanism could take place, with oocytes progressively losing their adhered granulosa cells to the intermediate stage ($C^{+/-}$) and from this to the denuded state (C^-). Both hypotheses are consistent with the observation that while C^+ oocytes exhibit a significant post-thaw decrease, $C^{+/-}$ oocyte numbers are relatively unaffected by cryopreservation (although in the gradual denuding mechanism these oocytes would have derived from the C^+ state).

Oocytes derived from large and small antral follicles show different TZPs-Act patterns, suggesting that changes at the granulosa–oocyte interface may reflect their developmental stage. Our hypothesis, that in antral follicles the C^- class represents a commitment to the apoptotic pathway, is consistent with the fact that the C^{A-} class exhibits a similarly low TZPs-Act density in all experimental groups. This further suggests that these oocytes may already be compromised from the start. Regarding small antral follicles, the high density of TZPs-Act in the C^{A-} class may support the hypothesis that granulosa cell adhesion may be partially independent of cell interaction via TZPs-Act. In fact, granulosa-free oocytes derived from small antral follicles exhibit a TZPs-Act density higher than their granulosa-enclosed counterparts. As previously stated, TZPs-Act have been related to both cell adhesion and mediating bi-directional communication at the granulosa–oocyte interface (Albertini and Rider, 1994; Albertini *et al.*, 2001; Albertini and Barrett, 2003; Combelles *et al.*, 2004). The present results, by showing that denuded

oocytes exhibit high TZPs-Act density, may support the view that TZPs-Act are preferentially involved in cell communication at the granulosa–oocyte interface. Taking into account that TZPs-MT are also key structures in follicular cell interaction (Albertini *et al.*, 2001; Albertini and Barrett, 2003), future studies are required to elucidate the possible TZPs-Act/TZPs-MT interplay. Furthermore, additional functional studies are necessary in order to clarify the putative role of TZPs-Act in cell communication in the follicle.

Cryopreservation reduced TZPs-Act density, as proven by the decrease of the relative intensity of the microfilament signal at the zona pellucida region. However, in contrast to this global trend, post-thaw C^{A-} oocytes showed a similar TZPs-Act density to their fresh counterparts. While this at first sight may seem contradictory, it could be explained by the above-hypothesized shift from the granulosa-enclosed classes, with higher TZPs-Act density, to the granulosa-free one. This way, oocytes could become granulosa-free while maintaining a TZPs-Act density close to the initial configuration. Once again this suggests that granulosa cell adhesion may be partially independent of TZPs-Act-mediated cell interaction. Previous studies indicate that post-thaw C^+ oocytes derived from antral follicles have considerably lower maturation rates than their denuded counterparts (Sztejn *et al.*, 2000). In the present study, the clear decrease of TZPs-Act density observed in the post-thaw C^+ classes further suggests that the granulosa–oocyte cell adhesion status alone may not be indicative of the degree of cryo-injury exerted upon the oocyte. Our results thus not only support previous studies of immature COCS (Sztejn *et al.*, 2000; Ruppert-Lingham *et al.*, 2003), but also expand those findings by focusing on the importance of maintaining the post-thaw integrity of the granulosa–oocyte interface. Additional clarification of factors regulating granulosa cell adhesion and somatic–germ cell interaction is needed in order to improve our knowledge of this critical cellular interface.

As expected, DMSO was found to be more effective than glycerol as an ovarian tissue cryoprotectant. With the choice of these two cryoprotectants, widely regarded as opposites in terms of functional recovery of thawed ovarian tissue (Candy *et al.*, 1997; Newton and Illingworth, 2001), it was our purpose to test a wider range of possible cryo-induced injuries on oocyte–granulosa cell interactions. Accordingly, in this study, cryopreservation in DMSO was more effective than in glycerol in maintaining a higher post-thaw TZPs-Act density. This may be a consequence of DMSO's higher tissue permeability coefficient when compared to glycerol (Newton *et al.*, 1998). Furthermore, even exposure to glycerol without freezing was enough to produce a detrimental effect on the average number of retrieved oocytes as well as on the pattern of oocyte–granulosa cell adhesion, supporting data suggesting that glycerol has a low efficiency as an ovarian tissue cryoprotectant (Candy *et al.*, 1997; Newton and Illingworth, 2001; see also Amorim *et al.*, 2004). Our findings that exposure to either cryoprotectant solution without freezing significantly reduces TZPs-Act density when compared to fresh tissue seem to indicate that TZPs-Act are extremely sensitive structures easily disruptable by subtle

alterations on the granulosa–oocyte microenvironment. Reassuringly, a positive interaction between cryopreservation and both cryoprotectants was detected in terms of TZPs-Act density, positively accounting for the use of cryoprotectants in cryopreservation protocols. Further improvements of cryopreservation protocols, both at the freezing and cryoprotectant exposure stages, are still necessary to better preserve oocyte–granulosa cell interaction. The advantages of non-linear cooling protocols (Morris *et al.*, 1999) and of cryoprotectants that minimize ice formation during thawing remain to be assessed at the highly complex soma–germ cell interface.

In conclusion, this study shows that murine fully grown immature oocytes derived from antral follicles exhibit different patterns of granulosa cell adhesion and TZPs-Act density that may reflect the oocyte's developmental stage. Furthermore, both cryopreservation and cryoprotectant exposure compromised the integrity of the granulosa–oocyte interface, suggesting that further optimization of cryopreservation protocols is still required to curtail the disruption of cellular communication routes in the ovary.

Acknowledgements

The authors thank D.F.Albertini, A.Sanfins, P.Rodrigues and M.Rato for their critical reading of the manuscript. In addition, the authors also acknowledge the contribution of two referees for the revised manuscript. Partially funded by FCT (project POC-TI/ESP/43628/2000).

References

Albertini DF and Barrett SL (2003) Oocyte–somatic cell communication. *Reproduction* 61 (Suppl),49–54.

Albertini DF and Rider V (1994) Patterns of intercellular connectivity in the mammalian cumulus–oocyte complex. *Microsc Res Tech* 27,125–133.

Albertini DF, Combelles C, Benecchi E and Carabatsos MJ (2001) Cellular basis for paracrine regulation of ovarian follicle development. *Reproduction* 121,647–653.

Amorim CA, Rondina D, Rodrigues AP, Gonçalves PB, de Figueiredo JR and Giorgetti A (2004) Cryopreservation of isolated ovine primordial follicles with propylene glycol and glycerol. *Fertil Steril* 81,735–740.

Anderson E and Albertini DF (1976) Gap junctions between the oocyte and companion follicle cells in the mammalian ovary. *J Cell Biol* 71,680–686.

Buccione R, Schroeder AC and Eppig JJ (1990) Interactions between somatic cells and germ cells throughout mammalian oogenesis. *Biol Reprod* 43, 543–547.

Candy CJ, Wood MJ and Whittingham DG (1997) Effect of cryoprotectants on the survival of follicles in frozen mouse ovaries. *J Reprod Fertil* 110,11–19.

Carabatsos M, Sellitto C, Goodenough D and Albertini D (2000) Oocyte–granulosa cell heterologous gap junctions are required for the coordination of nuclear and cytoplasmic meiotic competence. *Dev Biol* 226,167–179.

Combelles C and Albertini D (2003) Assessment of oocyte quality following repeated gonadotropin stimulation in the mouse. *Biol Reprod* 68,812–821.

Combelles C, Carabatsos MJ, Kumar TR, Matzuk MM and Albertini DF (2004) Hormonal control of somatic cell oocyte interactions during ovarian follicle development. *Mol Reprod Dev* 69,347–355.

Correia SC, Nogueira D, Martins O, Gomes JE, Arnold C, Cortvrindt R, Cidadão AJ, Sá-Melo P, Plancha CE and Smits J (1999) Follicular viability after ovarian tissue and follicle cryopreservation. Poster and oral communication European Society of Human Reproduction and Embryology—ESHRE Campus 99, Kilpisjärvi, Finland.

Deng W and Lin H (2001) Asymmetric germ cell division and oocyte determination during *Drosophila* oogenesis. *Int Rev Cytol* 203,93–138.

Eppig J, Wigglesworth K and Pendola F (2002) The mammalian oocyte orchestrates the rate of ovarian follicular development. *Proc Natl Acad Sci USA* 99,2890–2894.

Gilchrist R, Nayudu P, Nowshari M and Hodges J (1995) Meiotic competence of marmoset monkey oocytes is related to follicle size and oocyte–somatic cell associations. *Biol Reprod* 52,1234–1243.

Gilchrist R, Ritter L and Armstrong D (2004) Oocyte–somatic cell interactions during follicle development in mammals. *Anim Reprod Sci* 82–83, 431–446.

Gook D, Edgar D and Stern C (1999) Effect of cooling rate and dehydration regimen on the histological appearance of human ovarian cortex following cryopreservation in 1, 2-propanediol. *Hum Reprod* 14,2061–2068.

Gook D, McCully B, Edgar D and McBain J (2001) Development of antral follicles in human cryopreserved ovarian tissue following xenografting. *Hum Reprod* 16,417–422.

Gougeon A (1996) Regulation of ovarian follicular development in primates: facts and hypotheses. *Endocr Rev* 17,121–156.

Hertig AT and Adams EC (1967) Studies on the human oocyte and its follicle. I. Ultrastructural and histochemical observations on the primordial follicle stage. *J Cell Biol* 34,647–675.

Hovatta O, Silye R, Krausz T, Abir R, Margara R, Trew G, Lass A and Winston R (1996) Cryopreservation of human ovarian tissue using dimethyl sulfoxide and propanediol-sucrose as cryoprotectants. *Hum Reprod* 11,1268–1272.

Matzuk M, Burns K, Viveiros M and Eppig J (2002) Intercellular communication in the mammalian ovary: oocytes can carry the conversation. *Science* 296,2178–2180.

Morris GJ, Acton E and Avery S (1999) A novel approach to sperm cryopreservation. *Hum Reprod* 14,1013–1021.

Motta PM, Makabe S, Naguro T and Correr S (1994) Oocyte follicle cells association during development of human ovarian follicle. A study by high resolution scanning and transmission electron microscopy. *Arch Histol Cytol* 57,449–460.

Newton H and Illingworth P (2001) In-vitro growth of murine pre-antral follicles after isolation from cryopreserved ovarian tissue. *Hum Reprod* 16,423–429.

Newton H, Fisher J, Arnold JR, Pegg DE, Faddy MJ and Gosden RG (1998) Permeation of human ovarian tissue with cryoprotective agents in preparation for cryopreservation. *Hum Reprod* 13,376–380.

Oktay K, Nugent D, Newton H, Salha O, Chatterjee P and Gosden RG (1997) Isolation and characterization of primordial follicles from fresh and cryopreserved human ovarian tissue. *Fertil Steril* 67,481–486.

Pellicer A, Lightman A, Parmer TG, Behrman HR and De Cherney AH (1988) Morphological and functional studies of immature rat oocyte–cumulus complexes after cryopreservation. *Fertil Steril* 50,805–810.

Plancha CE (1996) Cytokeratin dynamics during oocyte maturation in the hamster requires reaching of metaphase I. *Differentiation* 60,87–98.

Plancha CE and Albertini DF (1994) Hormonal regulation of meiotic maturation in the hamster oocyte involves a cytoskeleton-mediated process. *Biol Reprod* 51,852–864.

Ruppert-Lingham C, Paynter S, Godfrey J, Fuller B and Shaw R (2003) Developmental potential of murine germinal vesicle stage cumulus–oocyte complexes following exposure to dimethylsulphoxide or cryopreservation: loss of membrane integrity of cumulus cells after thawing. *Hum Reprod* 18,392–398.

Simon A, Goodenough D, Li E and Paul D (1997) Female infertility in mice lacking connexin 37. *Nature* 385,525–529.

Sztein JM, O'Brien MJ, Farley JS, Mobraaten LE and Eppig JJ (2000) Rescue of oocytes from antral follicles of cryopreserved mouse ovaries: competence to undergo maturation, embryogenesis, and development to term. *Hum Reprod* 15,567–571.

Wang X, Chen H, Yin H, Kim SS, Lin Tan S and Gosden RG (2002) Fertility after intact ovary transplantation. *Nature* 415,385.

Zamboni L (1974) Fine morphology of the follicle wall and follicle cell–oocyte association. *Biol Reprod* 10,125–149.

Submitted on January 5, 2004; resubmitted on November 17, 2004; accepted on January 13, 2005